

Temperature Transformation of Dopant Spectra in Incommensurate Biphenyl[†]Artur Suisalu,[‡] Margus Jänes,[§] and Jaak Kikas^{*,§}*Institute of Physics, University of Tartu, Riia Street 142, 51014 Tartu, Estonia, and
Department of Physics, University of Tartu, Tähe Street 4, 51010 Tartu, Estonia**Received: February 4, 2004; In Final Form: May 6, 2004*

Phosphorescence spectra of phenanthrene and pyrene dopants in biphenyl are recorded at temperatures varied from 5 to 45 K. The spectra show an abrupt change at 17 K characteristic for the first-order phase transition. By further increase of the temperature, a continuous convergence of two Lorentzian spectral components is observed near 40 K. For the pyrene probe, the symmetrical splitting of the spectra exhibits a characteristic critical behavior, yielding a critical exponent of 0.41 and critical temperature 39.6 K for the incommensurate–commensurate phase transition. The phenanthrene probe does not precisely reflect the bulk structure of incommensurate biphenyl due to preferred distribution of phenanthrene guest molecules within domain boundaries.

1. Introduction

The absorption, fluorescence, and phosphorescence spectra of impurity molecules in biphenyl crystals at low temperatures show multiplet structure^{1–5} split by 10–30 cm^{−1}. An anomalous interconversion in spectral doublets of phenanthrene in solid biphenyl at temperatures above 10 K was for the first time described by Hochstrasser and Small.² For the dilute mixed crystal of protobiphenyl in deuteriobiphenyl⁴ it was suggested that biphenyl crystals may undergo a structural transformation during cooling to 4.2 K. The first clear experimental evidence on a gradual structural change of neat crystal of biphenyl came from the temperature-dependent Raman study.⁶ Also, ENDOR measurements^{7,8} showed additional low-temperature magnetic resonances, expected on the basis of a structure having half a molecule of biphenyl per asymmetric unit. Subsequently, two reports on Raman⁹ and low-field EPR¹⁰ have appeared, which further characterized the nature of the phase transitions near 40 and 17 K.

Single-crystal X-ray and neutron diffraction analyses have been performed on protio- and deuteriobiphenyl, and it has been proved that from room temperature down to 40 K the symmetry of biphenyl crystal is described by the centrosymmetric space group $P2_1/a$ with $Z = 2$.^{11,12} Between 40 and 17 K, the high-temperature structure approximately doubles along the b -axis (coinciding with the b^* -axis of reciprocal lattice) and the crystal shows incommensurate modulations in both the a^* and b^* directions of reciprocal lattice.¹³ At 17 K a partial lock-in transition occurs at which the modulation in the a^* direction vanishes, but that along b^* remains, and the structure tends toward an ordering with the space group Pa with $Z = 4$.^{14,15} These phases (commensurate phase CI , and two incommensurate phases $ICII$ and $ICIII$) and the related phase transitions have been afterward extensively studied by different methods, such as neutron¹⁶ and Raman¹⁷ scattering, adiabatic calorimetry,¹⁸ NMR,^{19,20} and EPR.^{21,22} Intensive experimental and many

theoretical studies^{23–26} of biphenyl make it the best-understood incommensurate molecular crystal.

It is our aim to demonstrate in this paper that the temperature-induced transformation of inhomogeneous spectra of an optical probe can reflect structural changes of the biphenyl crystal, if there is good enough accommodation of guest (probe) molecules into the host (biphenyl) crystal and close to the pure biphenyl values for the critical parameters can be obtained as well. Phenanthrene and pyrene probes were chosen, because they show well-structured luminescence spectra^{1–3} with large Debye–Waller factors. The torsional rigidity of the dopant molecules used reduces the influence of doping on the lattice dynamics due to strong localization of the probe torsion at impurity (out of resonance with the soft biphenyl torsion).²⁷ It was our expectation that due to a weaker interaction with the biphenyl torsion (linear and quadratic electron–phonon coupling both weak) the zero-phonon transition in the present probes is less sensitive to the temperature increase; in particular, the Stokes' losses related to the soft mode of biphenyl are reduced. In our earlier study of spectral hole burning^{28,29} in chlorin-doped biphenyl, we encountered a very sharp temperature dependence of the homogeneous zero-phonon lines. This was the reason our following studies on the influence of the host structural transformations on the chlorin spectra were performed in the pressure domain.^{30,31} It is demonstrated in what follows that the probes used in this work (especially pyrene) are more favorable and enabled us to study these transformations in the temperature domain as well.

2. Experimental Section

Spectroscopic measurements were carried out on a spectrometer based on a double-grating LOMO DFS-24 monochromator (linear dispersion 4.5 Å/mm) equipped with an Andor CCD-camera DU420-BU. The central slit of the monochromator was removed, and the CCD camera replaced the output slit. Typical spectral resolution of 0.02 nm was used for recording low-temperature phosphorescence spectra of doped crystals in a liquid ⁴He cryostat. The temperature was stabilized by regulating the flow rate of cold ⁴He gases into the sample compartment of the cryostat. The stability of temperature was 0.2 or 0.3 deg in

[†] Part of the special issue "Gerald Small Festschrift".

^{*} To whom correspondence should be addressed. E-mail: jaak.kikas@ut.ee.

[‡] Institute of Physics, University of Tartu.

[§] Department of Physics, University of Tartu.

the temperature range 5–25 or 25–45 K, correspondingly. Spectra were recorded in the range 5–45 K by 1-deg steps. Note that this allows a much more detailed study of spectral transformations compared to the aforementioned pressure-domain experiments,^{30,31} where a relatively much larger pressure step was used on technical reasons.

The $^3B_2 \rightarrow ^1A_1$ phosphorescence at 467.7 nm of the phenanthrene-doped biphenyl crystal was excited in the 1400 cm^{-1} -vibronic region of the $^1A_1 \rightarrow ^1A_1$ absorption (350.3 nm) with a N_2 -laser (337 nm). The excitation of the $^3B_{1u} \rightarrow ^1A_g$ phosphorescence at 596 nm of pyrene-doped biphenyl was close to the second singlet–singlet electronic transition of $^1A_g \rightarrow ^1B_{1u}$ using the UV line (351.4 nm) of a Coherent Innova Ar^+ -laser. A multiple-Lorentzian line fitting and two-dimensional contour plot of stacked fixed-temperature phosphorescence spectra were performed using Origin 6.0 graphical interface.

Note that the choice of phosphorescence (instead of fluorescence) for monitoring structural changes in biphenyl was made on technical reasons. The 0–0 fluorescence bands of phenanthrene and pyrene probes, located at 350 and 375 nm, respectively, are well beyond the blue limit of our spectrometer (400 nm). Usage of vibronic fluorescence at longer wavelengths, however, obscures the spectral resolution due to broadening and overlap of vibronic levels. Our data on comparison of probe (Zn–chlorin) fluorescence and phosphorescence in biphenyl (unpublished) demonstrated, however, a good correspondence between the main spectral features in fluorescence and phosphorescence.

Purum grade biphenyl (>98%, HPLC), phenanthrene (~97%, GC), and pyrene (~97%, UV) were purchased from Fluka AG. Biphenyl was purified twice by vacuum sublimation until any traces of naphthalene, fluorene, and phenanthrene emission disappeared from its luminescence spectra. Less than 10^{-4} mol fraction of phenanthrene or pyrene were dissolved subsequently in the purified biphenyl at 5 deg above the melting point of biphenyl (69 °C) in a quartz capillary tube with 3 mm inner diameter. Then 10 mm-length diluted mixed crystals with minor cracks were grown from the melt by gradually lowering the temperature at the rate of -2.75 deg/h. To check possible deviations from a spatially uniform distribution of probes due to the limited solid solubility of guest molecules in biphenyl ($\approx 10^{-3}$ M was reported for phenanthrene³²) the distribution of guest molecules was inspected by the measurement of luminescence intensity as well as spectra along the capillary tube (in the direction of temperature gradient) by 1 mm step. No zone refining effect was found.

To confirm that we have a diluted mixed crystal and the guest molecules are homogeneously distributed in the host, we also have measured phosphorescence decay curves at 5 and 45 K. We got excellent single-exponential decays with time constants of 3.02 and 2.93 s for the phenanthrene-doped biphenyl at the above-mentioned temperatures and, correspondingly, 0.56 and 0.54 s for the pyrene-doped biphenyl. These values agree well with the previous data of 2.8 s for phenanthrene in biphenyl³³ and 0.5 s for pyrene in fluorene³⁴ and correspond to the average lifetime values of the lowest triplet state due to fast spin–lattice relaxation³³ at these temperatures. No nonexponential behavior due to triplet–triplet energy transfer was detected, found previously for phenanthrene in biphenyl at much higher doping concentrations.³⁵

3. Results and Discussion

The 0,0-phosphorescence band of both probes displays a multiline structure at 5 K, as seen previously: a doublet structure

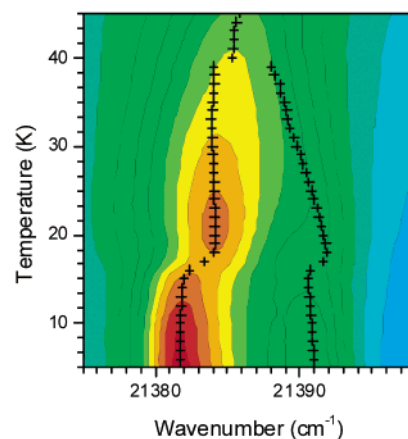


Figure 1. 2D frequency–temperature plot (isointensity curves) of phenanthrene (0–0)-phosphorescence intensity $I(\nu, T)$ in biphenyl. Crosses: the peak positions of spectral components obtained from the multipeak fitting of spectra at a fixed temperature.

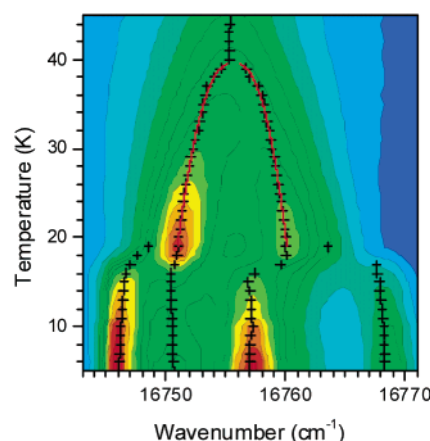


Figure 2. 2D frequency–temperature plot (isointensity curves) of pyrene (0–0)-phosphorescence intensity $I(\nu, T)$ in biphenyl. Crosses: the peak positions of spectral components obtained from the multipeak fitting of spectra. Solid red curves: fits of data points in incommensurate phase *ICII* according to eq 1 with the least-squares fit values $\nu_0 = 16\,755.4$ cm^{-1} , $\alpha = 0.0053$ cm^{-1}/K , $\Delta = 11.9$ cm^{-1} , $T^* = 39.6$ K, and $\beta = 0.41$.

for phenanthrene^{1,2} and a quartet structure for pyrene.^{2,3} An excellent collection of the available data on site splitting one can find in Table 2 of ref 5. At the highest temperature used, 45 K, the 0,0-band of phosphorescence contains a single line with the fwhm 11 cm^{-1} for the both guest molecules. The two-dimensional (frequency–temperature) isointensity plot of the phenanthrene- and pyrene-stacked phosphorescence spectra for temperatures from 5 to 45 K are depicted in Figure 1 and Figure 2, correspondingly. As can be seen, both probe molecules show common features in the temperature-dependent spectra: an abrupt shift of spectral lines at 17 K corresponding to the first-order phase transition and a gradual convergence of two spectral components at 40 K approaching the second-order phase transition. However, guest-specific details reflecting local structure of doped crystals can be distinguished as well. First, the number of spectral sites (lines) in the phase *ICIII* is different for different probes—two for phenanthrene and four for pyrene probes. Second, in the higher-temperature incommensurate phase, *ICII*, there remains a spectral doublet for both probes, but in the case of phenanthrene the high-frequency component of the doublet is strongly reduced in intensity.

To get quantitative data on the temperature-dependent spectra we applied multiline fitting procedure. The multiline guest

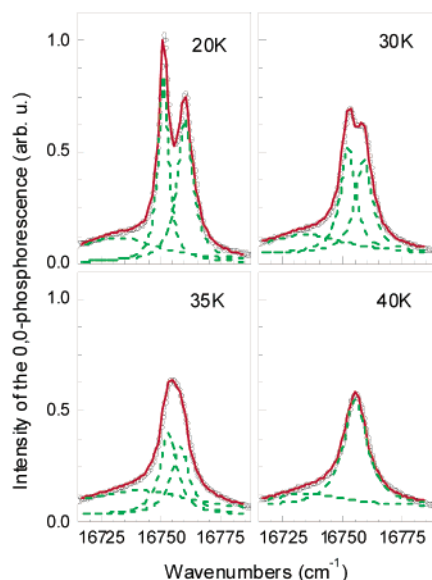


Figure 3. Multi-Lorentzian fitting of the purely electronic (0–0)-band and phonon-wing of pyrene in incommensurate phase *ICII* of biphenyl. The red solid curve represents the overall fit spectrum; dashed green curves represent the individual Lorentzian components, and a single Lorentzian is used to fit the contribution from phonon sidebands.

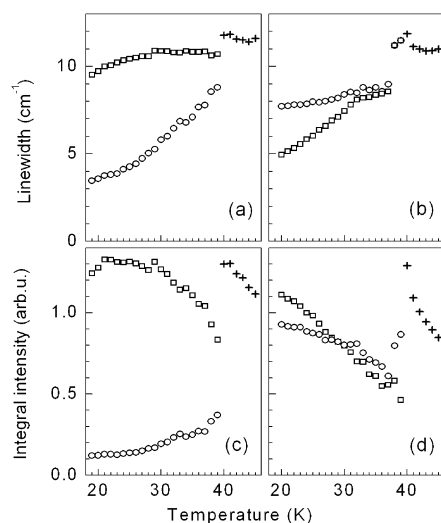


Figure 4. Temperature dependence of line widths (a, b) and integral intensities (c, d) of spectral lines in the (0–0)-bands of phenanthrene (a, c) and pyrene (b, d). Squares represent data of the low-frequency and circles represent high-frequency components in incommensurate phase *ICII*. Crosses represent data for the single line in commensurate phase *CI*.

spectra measured in phase *ICIII* of biphenyl cannot be well fitted by symmetric Lorentzian or Gaussian functions due to the asymmetry of individual spectral lines. Therefore, only the reliable data on line positions are depicted in Figures 1 and 2 and no speculation is made on the line broadening. Spectra measured in phases *ICII* and *CI* can be satisfactorily fitted to Lorentzian curves with a nonlinear baseline (Figure 3). The results of fitting are depicted in Figures 1 and 2 for the line positions and in Figure 4 for the line width and area. It is clearly seen that for phenanthrene-doped biphenyl the weak high frequency component is temperature-sensitive, while the strong low-frequency component is much broader and its spectral position and width do not depend on temperature. For pyrene-doped biphenyl, the temperature dependences of both spectral components are nearly symmetrical. Such a different behavior of two dopant molecules could be explained by assuming that

phenanthrene probe molecules are mostly located in nonperfect region of the biphenyl crystal where structural changes of the bulk crystal are less expressed. Here we recall the analogy with the doped isomorphous *p*-terphenyl crystal in the low-temperature ferroelastic phase: pentacene guest molecules are predominantly located in regular crystalline regions, while tetracene guest molecules mostly reside in domain boundaries.³⁶

The imperfections of incommensurate biphenyl in phase *ICII* are boundaries separating domains, which are alternatively modulated with one of the two different modulation wave-vectors. This “stripelike” structure of biphenyl disappears at the phase transition *ICII* → *ICIII*. Given that the probe positions freeze in at much higher temperatures compared to the formation of domain walls, the association of impurities with the domain boundaries, in fact, means the opposite—the phenanthrene probe governs (at least to some extent) the distribution of domain boundaries.

Assuming that the incommensurate modulation of the probe transition frequency depends linearly on the order parameter (torsion angle between the phenyl rings), the corresponding temperature dependence of line positions (location of edge singularities) can be expressed as²¹

$$\nu_{1,2} = \nu_0 + aT \pm \frac{\Delta}{2} \left(1 - \frac{T}{T^*}\right)^\beta \quad (1)$$

with $\Delta = 11.9 \text{ cm}^{-1}$. The splitting $\nu_1 - \nu_2$ of the spectral doublet converges to zero at $T^* = 39.6 \text{ K}$ following a critical power law with exponent $\beta = 0.41$ (Figure 2), with all the parameters obtained as fit values. Note that a very close value for the same exponent, 0.41, was obtained from EPR spectra²¹ of the naphthalene-*d*₈ probe in biphenyl-*h*₁₀, while a somewhat lower value of 0.35 ± 0.03 was found from bulk biphenyl-*d*₁₀ NMR measurements.²⁰ The obtained value for the critical temperature for the incommensurate (*ICII*)–commensurate (*CI*) phase transition is also pretty close to the values obtained by bulk methods^{9,18} for biphenyl-*h*₁₀. At temperatures above 40 K, there remains a single line much in common with what we observed for chlorin probe in *pressure* domain, where a low-pressure (incommensurate) multiplet converges to a single line at pressures above 180 MPa in the commensurate crystalline phase.³⁰ Within a limited temperature range of 40–45 K, the position of the line does not depend much on temperature—one can well assume that it shows a weak blue shift at a rate close to the value of $a = 0.0053 \text{ cm}^{-1}/\text{K}$ obtained for the temperature shift of the *mean* frequency of the spectral doublet in phase *ICII*.

4. Conclusions

We have demonstrated that optical spectra of pyrene and phenanthrene molecular probes in biphenyl reflect the transformations in the pure host compound. In particular, values for the commensurate–incommensurate transition temperature and for the corresponding critical exponent were obtained from the probe spectra, close to the “bulk” values from other methods. While showing common features, the two probes exhibit some differences as well, ascribed to the preferred location of phenanthrene in the domain walls. Extension of these studies into pressure domain is in progress and could complement the results we have obtained from temperature measurements. Recent IR studies with numerical simulation and group-theoretical analysis of biphenyl vibrations and their transformation with pressure³⁷ may be quite helpful within this context.

Acknowledgment. This work was supported by the Estonian Science Foundation under Grant No. 5544. We thank Dr. N. Palm for purification of biphenyl.

References and Notes

- (1) Hochstrasser, R. M.; Small, G. J. *J. Chem. Phys.* **1966**, *45*, 2270.
- (2) Hochstrasser, R. M.; Small, G. J. *J. Chem. Phys.* **1968**, *48*, 3612.
- (3) Bree, A.; Vilkos, V. V. B. *Spectrochim. Acta, Part A: Mol. Spectrosc.* **1971**, *272*, 333.
- (4) Hochstrasser, R. M.; McAlpine, R. D.; Whiteman, J. D. *J. Chem. Phys.* **1973**, *58*, 5078.
- (5) Hochstrasser, R. M.; Scott, G. W.; Zewail, A. H.; Fuess, H. *Chem. Phys.* **1975**, *11*, 273.
- (6) Friedman, P. S.; Kopelman, R.; Prasad, P. N. *Chem. Phys. Lett.* **1974**, *48*, 15.
- (7) Brenner, H. C.; Hutchison, C. A., Jr.; Kemple, M. D. *J. Chem. Phys.* **1974**, *60*, 2180.
- (8) Hutchison, C. A., Jr.; McCann, V. H. *J. Chem. Phys.* **1974**, *61*, 820.
- (9) Bree, A.; Edelson, M. *Chem. Phys. Lett.* **1977**, *46*, 500.
- (10) Cullick, A. S.; Gerkin, R. E. *Chem. Phys.* **1977**, *23*, 217.
- (11) Charbonneau, G.-P.; Délugeard, Y. *Acta Crystallogr.* **1976**, *B32*, 1420.
- (12) Charbonneau, G.-P.; Délugeard, Y. *Acta Crystallogr.* **1977**, *B33*, 1586.
- (13) Cailleau, H.; Moussa, F.; Mons, J. *Solid State Commun.* **1979**, *31*, 521.
- (14) Cailleau, H.; Baudour, J. L.; Zeyen, C. M. E. *Acta Crystallogr.* **1979**, *B35*, 426.
- (15) Baudour, J. L.; Sanquer, M. *Acta Crystallogr.* **1983**, *B39*, 75.
- (16) Moussa, F.; Launois, P.; Lemée, M. H.; Cailleau, H. *Phys. Rev.* **1987**, *B36*, 8951.
- (17) Lemée-Cailleau, M. H.; Girard, A.; Cailleau, H.; Délugeard, Y. *Phys. Rev.* **1992**, *B45*, 12682.
- (18) Saito, K.; Atake, T.; Chihara, H. *Bull. Chem. Soc. Jpn.* **1988**, *61*, 679.
- (19) Liu, S.-B.; Conradi, M. S. *Phys. Rev. Lett.* **1985**, *54*, 1287.
- (20) von Laue, L.; Ermark, F. Götzhäuser, A.; Haeberlen, U.; Häcker, U. *J. Phys.: Condens. Matter* **1996**, *8*, 3977.
- (21) Veron, A.; Emery, J.; Spiesser, M. *J. Phys. I Fr.* **1994**, *4*, 1705.
- (22) Veron, A.; Emery, J.; Spiesser, M. *J. Phys. Chem. Solids* **1996**, *57*, 1201.
- (23) Benkert, C.; Heine, V. *Phys. Rev. Lett.* **1987**, *58*, 2232.
- (24) Parlinski, K. *Phys. Rev.* **1989**, *B39*, 488.
- (25) Lenstra, A. T. H.; Van Alsenoy, C.; Verhulst, K.; Geise, H. J. *Acta Crystallogr.* **1994**, *B50*, 96.
- (26) Corish, J.; Morton-Blake, D. A.; O'Donoghue, F.; Baudour, J. L.; Beniere, F.; Toudic, B. *J. Mol. Struct. (THEOCHEM)* **1995**, *358*, 29.
- (27) Yamamura, Y.; Saito, K.; Sorai, M.; Ikemoto, I. *J. Phys. Soc. Jpn.* **1998**, *67*, 1649.
- (28) Suisalu, A.; Zazubovich, V.; Kikas, J.; Friebe, J.; Friedrich, J. *Europhys. Lett.* **1998**, *44*, 613.
- (29) Zazubovich, V.; Suisalu, A.; Kikas, J. *Phys. Rev.* **2001**, *B64*, 104203.
- (30) Zazubovich, V.; Suisalu, A.; Leiger, K.; Laisaar, A.; Kuznetsov, A.; Kikas, J. *Chem. Phys.* **2003**, *288*, 57.
- (31) Kikas, J.; Suisalu, A.; Laisaar, A.; Kuznetsov, A. *Low Temp. Phys.* **2003**, *9–10*, 801.
- (32) Cullick, A. S.; Gerkin, R. E. *J. Chem. Phys.* **1977**, *67*, 1427.
- (33) Antheunis, D. A.; Botter, B. J.; Schmidt, J.; Verbeek, P. J. F.; van der Waals, J. H. *Chem. Phys. Lett.* **1975**, *36*, 225.
- (34) Sixl, H.; Schwoerer, M. *Z. Naturforsch.* **1970**, *25a*, 1383.
- (35) Tean, S.; Gondo, Y. *Chem. Phys. Lett.* **1986**, *123*, 441.
- (36) de La Riva, C.; Kryshi, C.; Trommsdorff, H. P. *Chem. Phys. Lett.* **1994**, *227*, 13.
- (37) Zhuravlev, K. K.; McCluskey, M. D. *J. Chem. Phys.* **2002**, *117*, 3748.